A high-resolution neutron powder diffraction study of ammonia dihydrate ($ND_3 \cdot 2D_2O$) phase I

A. D. Fortes,[a] I. G. Wood, J. P. Brodholt, M. Alfredsson, and L. Vočadlo
Department of Earth Sciences, University College London, Gower Street, London WC1E 6BT, United Kingdom

G. S. McGrady
Department of Chemistry, University of New Brunswick, Fredericton, New Brunswick E3B 6E2, Canada

K. S. Knight
ISIS Facility, Rutherford Appleton Laboratory, Chilton, Didcot, Oxfordshire OX11 0QX, United Kingdom

(Received 1 July 2003; accepted 25 August 2003)

We have measured the thermal expansivity of ammonia dihydrate ($ND_3 \cdot 2D_2O$) phase I from 4.2 to 174 K at ambient pressure, and the incompressibility at 174 K from 0 to 0.45 GPa, using time-of-flight neutron powder diffraction. The unit cell volume as a function of temperature, $V(T)$, was fitted with a Grüneisen approximation to the zero-pressure equation of state (with the lattice vibrational energy calculated from a double-Debye model fitted to heat capacity data) having the following parameters at zero pressure and temperature: $V_{0,0}=356.464\pm0.005$ Å^3, $(K_{0,0}/\gamma)=7.163\pm0.024$ GPa, and $K'_{0,0}=5.41\pm0.33$ (where $V_{P,T}$ is the unit cell volume at pressure P and temperature T, $K_{P,T}$ is the isothermal bulk modulus, $K'_{P,T}$ is its first pressure derivative, and γ is the Grüneisen ratio). The two Debye temperatures are $\theta_D^A=165\pm3$ K and $\theta_D^B=729\pm4$ K. The unit cell volume at 174 K as a function of pressure, $V(P)$, was fitted with a third-order Birch–Murnaghan equation of state having the following parameters: $V_{0,174}=365.69\pm0.16$ Å^3, $K_{0,174}=7.02\pm0.25$ GPa, and $K'_{0,174}=9.56\pm1.28$. The volume thermal expansion coefficient, α_V, at 174 K and atmospheric pressure is 281.3×10^{-6} K^{-1}. The proton disorder manifested at high homologous temperatures is seen to be frozen in, on the time scale of these experiments, down to 4.2 K. A high-pressure polymorph of ammonia dihydrate was observed following melting of the sample at 179 K and 0.46 GPa. © *2003 American Institute of Physics.* [DOI: 10.1063/1.1619371]

I. INTRODUCTION

Ammonia dihydrate (ADH) was first identified by Rollet and Vuillard.[1] The crystal structure of the ambient pressure phase (ADH I) was studied by x-ray powder diffraction and inferred to be proton ordered (on the basis of infrared spectroscopy), probably in space group $P2_12_12_1$ at 100 K.[2] This was in agreement with earlier calorimetric measurements, which found no evidence of hydrogen bond disorder at very low temperatures.[3] However, neutron powder diffraction established that ADH I is cubic (space group $P2_13$) and disordered at 150 K.[4] We recently proposed a solution to this problem wherein paraelectrically disordered cubic ADH I transforms to antiferroelectrically ordered orthorhombic ADH upon cooling below ~140 K.[5]

The pressure and temperature dependencies of the molar volume of ADH I have never been measured previously, but are of paramount importance to planetary scientists. Based on the cosmic abundance of ammonia it has been suggested that the icy moons in the outer Solar System may contain up to 15 wt% NH_3.[6] An ammonia–water solution of this stoichiometry will crystallize a mixture of ice Ih + ADH I:[7,8] intermediate-sized icy moons, such as Rhea (a moon of Saturn), could contain a layer of ADH I up to 250 km deep beneath an ice Ih crust 140 km thick.[5] In order to model the internal structure and thermal history of these icy moons, accurate values for the thermal expansivity and incompressibility of ADH I are required.[9,10] We recently published the results of *ab initio* calculations on ADH,[5] reporting the equation of state in the athermal limit, and consequently have an interest in comparing these results with experimental data.

There are therefore a number of questions regarding ADH I that we wish to be addressed. What is the thermal expansivity of ADH I throughout its temperature stability field? What is the incompressibility of ADH I? Does ADH I undergo an order–disorder transition near 140 K? In order to answer these questions we have carried out a neutron powder diffraction study upon perdeuterated ADH I. These experiments were done using the time-of-flight method on the high resolution powder diffractometer (HRPD) beamline at the ISIS neutron spallation source (Rutherford Appleton Laboratory, Chilton, Oxfordshire, U.K.).[11] The unparalleled resolution of this instrument ($\Delta d/d \sim 4\times10^{-4}$ in the backscattering detectors) makes it ideal for the rapid and accurate determination of lattice parameters (for measuring thermal expansivity and incompressibility), and for the detection of very fine Bragg peak splittings concomitant with the proposed order–disorder transition.

In addition to measuring the properties of ADH I, we also wished to observe the phase transition to a denser poly-

[a]Electronic mail: andrew.fortes@ucl.ac.uk

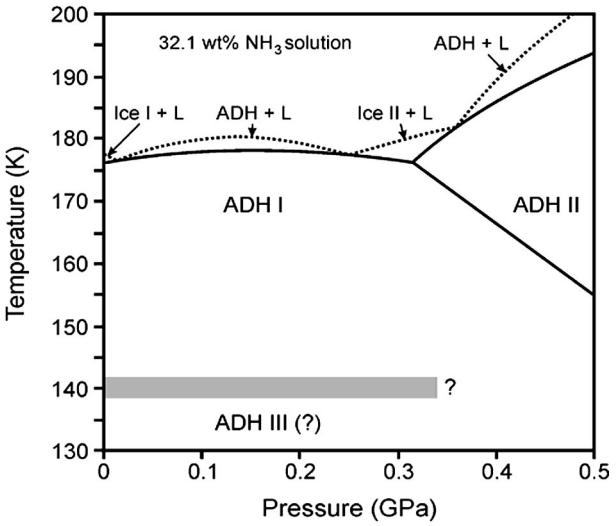

FIG. 1. The expected phase relations in ammonia dihydrate at low pressures (Ref. 5).

morph of ammonia dihydrate (ADH II). This transition has been seen previously in piston compression experiments[12] and by neutron powder diffraction;[13] see Fig. 1.

In the following section (Sec. II) we describe our sample preparation method and data acquisition strategy: ADH is notoriously difficult to crystallize[2,3,14] since it tends to form a glass when supercooled below its melting point (the protonated isotopomer melts incongruently at 176.16 K),[3] and then disproportionates into ammonia monohydrate+ice. We therefore pay particular attention to describing the recipe that was followed to produce crystalline ADH I. In Sec. III we present our results, reporting the pressure and temperature dependence of the unit cell volume and our observations regarding the structure at low temperatures.

II. EXPERIMENT

A. Sample preparation

A liquid solution of the correct stoichiometry ($33\frac{1}{3}$ mol% ND_3) was prepared by mixing an appropriate volume of condensed heavy ammonia (Aldrich Chemicals Co., 99 atom % D) with heavy water (Aldrich Chemicals Co., 99 atom % D). This liquid was stored in a refrigerator for approximately three months prior to use.

An aluminum slab-can with vanadium windows was employed for the ambient pressure experimental runs. The sample cavity was loosely padded with silica wool to ensure nucleation of a good powder from the liquid, and $ND_3 \cdot 2D_2O$ solution was dripped onto the wool until the space was filled. The can was sealed, attached to a cryostat center stick, and quenched to 77 K in a nitrogen dewar. This assembly was then placed in a vanadium-tailed helium cryostat pre-cooled to 50 K and allowed to thermally equilibrate before being warmed to 174 K. In order to produce crystalline ADH the temperature was cycled across the melting point a number of times according to the recipe of Bertie and Shehata;[2] the temperature was ramped up from 174 to 179 K over 15 minutes, and then reduced to 174 K over 3 minutes. The cycle was repeated four times (72 minutes in total), and the sample was then kept at 174 K for ~20 hours before being placed in the neutron beamline.

For the high-pressure experimental runs a cylindrical aluminum gas pressure vessel was used. Once again, silica wool was utilized as a multinucleator and liquid $ND_3 \cdot 2D_2O$ was poured into the sample space. The can was sealed with a nominal pressure of ~500 bar of He gas. As pressure was released following an offline pressure test the sample was observed to boil, apparently outgassing ammonia vapor from solution. This altered the stoichiometry from ~33 mol% ND_3 to ~29 mol% ND_3, resulting in the crystallization of a significant amount of ice (~12.5 wt%) along with ADH.

The same temperature cycling process was used to crystallize ADH in the pressure can using a second vanadium-tailed helium cryostat with the sample held at ~400 bar. However, the time required was changed to account for the increased thermal inertia of the pressure can: the temperature was ramped up from 174 to 179 K over one hour, and then reduced to 174 K over 15 minutes. The cycle was repeated four times (5 hours total), and the sample was then held at 174 K for ~12 hours before being placed in the neutron beamline.

In both sample environments this process resulted in the formation of a good crystalline powder of ADH phase I.

B. Data acquisition

For the ambient pressure experiments, it was found that diffraction patterns suitable for the accurate determination of lattice parameters (i.e., with standard errors of order few $\times 10^{-5}$ Å) could be collected in approximately 10 minutes from the backscattering and 90° detector banks (e.g., Fig. 2). We therefore collected data at temperature intervals of 2 K while cooling the sample from 174 to 4.2 K; a cooling rate of 8 K hr^{-1}, allowing for 5 minutes of thermal equilibration before data collection at each temperature point. Data were collected for ~1 hour at 4.2 K in order to allow for more detailed structural refinement (see Table I). Since no obvious signs of the expected ordering[5] were observed during this period, the sample was taken offline and held at 120 K for ~36 hours in an effort to promote the ordering transformation. This sample was then returned to the beamline and cooled to 40 K. Finally, diffraction patterns suitable for high quality structure refinement (~100 minutes per spectrum) were collected at 20 K intervals upon warming from 40 to 160 K. This latter data set is hereafter referred to as the post-annealing data, and the run of spectra at 2 K intervals as the pre-annealing data set.

The high-pressure sample was introduced to the neutron beamline under a nominal pressure of 0.041 GPa. We found that 15 minutes was an adequate period of time to accurately determine lattice parameters from the 90° detectors. The use of this detector bank enables most of the scattering from the pressure vessel to be collimated out. The pressure was stepped up (using helium as the pressure transmitting medium) in intervals of ~0.05 GPa to the maximum rated pressure of the aluminum cell (~0.46 GPa). Diffraction patterns confirmed the earlier observation of Loveday *et al.*[13] that he-

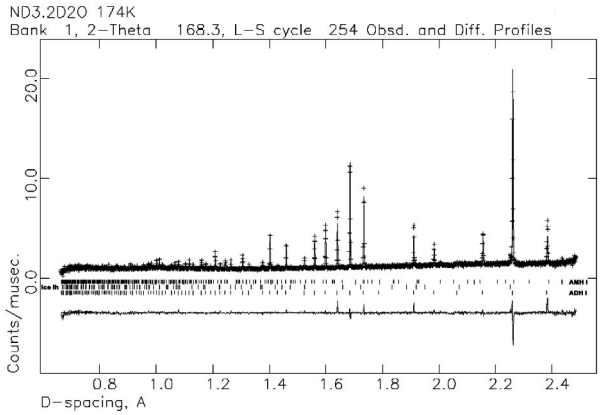

FIG. 2. Observed and calculated profiles for the diffraction pattern acquired at ambient pressure, 174 K, including difference profile (bottom). Tick-marks, from the top down, show the positions of reflections due to AMH I, ice Ih, and ADH I.

lium does not penetrate the ADH I structure. At 0.35 GPa there was a drop in pressure, and the Bragg peaks of ice Ih were replaced by reflections due to ice IX. This solid persisted as an accessory phase up to the maximum pressure investigated. Although not the equilibrium phase under the applied P-T conditions, the transition from ice Ih to ice IX has been seen in the 0.35–0.40 GPa pressure range below ~170 K previously;[15,16] however, it is known that the use of helium gas as a pressure medium inhibits the formation of ices III, V, and IX in favor of a helium hydrate with the ice II structure.[17] We conclude that the presence of ammonia dihydrate may have a preferential influence on the nucleation of ice IX with respect to helium-stuffed ice II, in spite of the observation by Londono *et al.*,[17] that they were unable to crystallize phases other than helium hydrate even when using specialized nucleating agents.

The anticipated phase transition to ADH II[12,13] had not occurred at 0.46 GPa, so the sample was warmed by 5 K. The sample promptly melted to a slurry containing ice IX crystals in ammonia–water slush. When cooled back to 174 K, new Bragg peaks appeared along with those of ice IX over a period of ~4 hours. Diffraction data were collected from this new polyphase mixture for ~11 hours at 174 K. The sample was then cooled in 5 K steps to 140 K, quenched to ~110 K and subsequently decompressed to ~500 bar, but the high-pressure peaks persisted, albeit with a considerable degree of strain broadening when the pressure was completely released. Our opinion is that we initially compressed ADH I *metastably* into the stability field of ADH II, but did not apply a great enough overpressure to make the phase transition occur. After melting, *stable* ADH II crystallized which was able to persist metastably in the stability field of ADH I when cooled and decompressed. Analysis of the data from the high-pressure phase is in progress; the structures of both ADH II and phase II of ammonia monohydrate (AMH II, another probable component of the multiphase mixture) are not known at present.

C. Refinement

The cell parameter of ADH I as a function of temperature was extracted from the pre-annealing data set using the ''cell and intensity least squares'' (CAILS) utility[18] in CCSL (the Cambridge Crystallography Subroutine Library).[19] Rietveld multiphase structure refinements of the post-annealing and high-pressure time-of-flight spectra were made using the GSAS package.[20] The ADH I structure was refined from the cubic cell of Loveday and Nelmes.[4] At ambient pressure, the minor phases coexisting with ADH I were successfully fitted with the structures of ice Ih[21] and ammonia monohydrate (AMH phase I).[4] At each temperature, only

TABLE I. Results of the isotropic structure refinement at 4.2 K. Bond lengths quoted are uncorrected for thermal motion.

Rietveld Powder statistics:	wRp=5.66% Rp=5.00%
Space group	$P2_13$
Lattice constant:	7.091 771(16) Å
Unit cell volume:	356.6680(14) Å

Atom	x	y	z	Occupancy	U_{iso} (×100) Å^2
O1	0.704 23(24)	0.704 23(24)	0.704 23(24)	1	0.73(7)
D1	0.759 28(47)	0.678 35(50)	0.577 01(56)	2/3	1.83(7)
O2	0.156 07(26)	0.156 07(26)	0.156 07(26)	1	1.31(9)
D2	0.238 80(26)	0.238 80(26)	0.238 80(26)	1	1.51(5)
D3	0.014 24(133)	0.207 23(89)	0.177 83(103)	1/3	2.42(17)
N1	0.379 44(20)	0.379 44(20)	0.379 44(20)	1	0.86(5)
D4	0.357 34(30)	0.357 83(23)	0.515 07(31)	1	2.57(6)

Selected bond lengths (Å)

N1–D4	0.9865(21)	D3···O1	1.682(9)
O1–D1	1.0000(35)	D2···N1	1.728(4)
O2–D2	1.0163(32)	D1···O2	1.766(4)
O2–D3	1.080(9)	D4···O1	2.311(3)
O2···N1	2.744(2)		
O1···O2	2.762(3)		
N1···O1	3.258(2)		

the unit cell dimensions of ice Ih and AMH I were refined; atomic coordinates were fixed at their literature values[4,21] and the temperature factors for each atomic species were set to the values refined from the ADH structure. The refinements of the ADH I structure were done with isotropic temperature factors (U_{iso} in Table I). It was found that an anisotropic refinement yielded minimal improvements in the fitting statistics, and also generated unphysical values for the atomic displacement parameters of the partially occupied deuteron sites.

In the high pressure experiment, ice Ih transformed to ice IX between 0.30 and 0.35 GPa: Cell parameters for this phase were refined on the basis of the fully ordered ice IX structure.[22] This is not strictly correct, since the observed structure of ice IX does exhibit a very small degree of partial disorder at 170 K; the probability of the weakly occupied deuteron sites being occupied is $\sim 4\%$.[17] Additional minor reflections were observed from the aluminum sample cans. Since the high-pressure runs were relatively short (10–20 minutes) the structure of ADH I was not refined, only the unit cell.

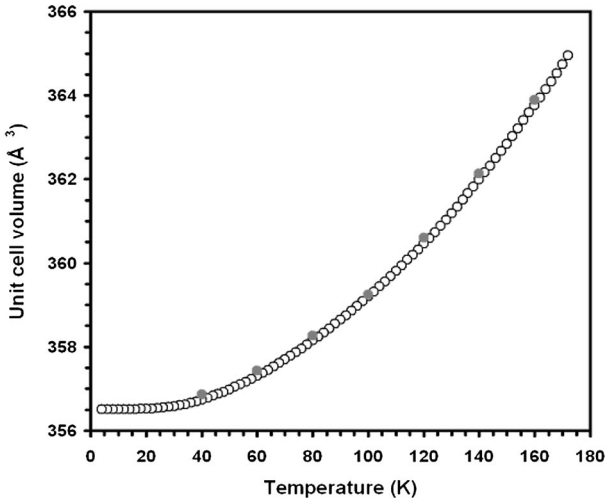

FIG. 3. Plot of refined unit cell volume against temperature at ambient pressure. The pre-annealing data set is shown as open circles, and the post-annealing data set as filled circles. The slight off set between the two can be explained in terms of small differences in the position of the sample (order 10^{-3} m) in the incident neutron beam.

III. RESULTS

A. Thermal expansivity

The pre-annealing data set consists of 85 data points at 2 K intervals, from which the lattice parameter was refined with a standard deviation on all points of 0.000 02 Å (Fig. 3). A second-order Grüneisen approximation to the zero pressure equation of state[23] [Eq. (1)] was fitted to the unit cell volumes found from the pre-annealing data set. In this approximation, the thermal expansion is considered equivalent to elastic strain such that

$$V(T)=V_{0,0}\left[1+\frac{E(T)}{Q-bE(T)}\right], \tag{1}$$

where $V_{0,0}$ is the unit cell volume at zero pressure and temperature, $b=\frac{1}{2}(K'_{0,0}-1)$ and $Q=(V_{0,0}K_{0,0}/\gamma)$. $K_{0,0}$ is the zero pressure and temperature isothermal bulk modulus, $K'_{0,0}$ is its first derivative with respect to pressure, and γ is the thermal Grüneisen parameter. The internal energy due to lattice vibrations, $E(T)$, is determined via a Debye model:[24]

$$E(T)=\frac{9nk_BT}{(\theta_D/T)^3}\int_0^{\theta_D/T}\frac{x^3}{e^x-1}dx, \tag{2}$$

where θ_D is the Debye temperature, n is the number of atoms per unit cell, and k_B is the Boltzmann constant; the integral term is evaluated numerically. This approach has been previously used with success on ''hard'' materials such as FeSi[25] and $KMgF_3$.[26]

When Eq. (1) is fitted to our $V(T)$ data the fit is excellent, both in terms of unit cell volume (Fig. 3) and the thermal expansivity (Fig. 4). Nevertheless, the elastic parameters resulting from the fit are not sensible ($K'_{0,0}=37.14$, for example) and the internal energy of the crystal yields values for the heat capacity which are very seriously at odds with experimental data.[3] Indeed it is impossible to achieve a good fit to the heat capacity data with a single Debye model (Fig. 5), and we therefore have little confidence in the parameters resulting from the fitting of Eq. (1) to $V(T)$ data as it stands. However, the appearance of the misfit to C_P suggests that ADH I differs radically from Debye (or Debye-type) solids in that there are two Debye moments with very different characteristic temperatures contributing to the internal energy of the crystal. It is a straightforward matter to fit a ''double-Debye'' function to the heat capacity data of Chan and Giauque,[3] which has the form

$$C=9nk_B\left[Xf\left(\frac{\theta_D^A}{T}\right)+Yf\left(\frac{\theta_D^B}{T}\right)\right], \tag{3}$$

where $f(\theta_D/T)$ is the Debye function and X and Y are mixing parameters. It should be noted that this is not intended to be an exact representation of the internal energy of the crystal since we are fitting to C_P data when we should be fitting

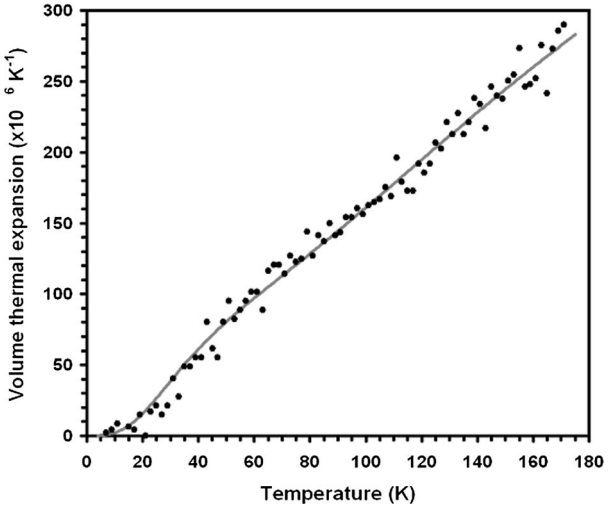

FIG. 4. Volume thermal expansivity as a function of temperature. The filled circles are numerical derivatives of the unit cell volumes with respect to temperature. The line is from the fitting of Eq. (1) using the double-Debye model fitted to C_P data.

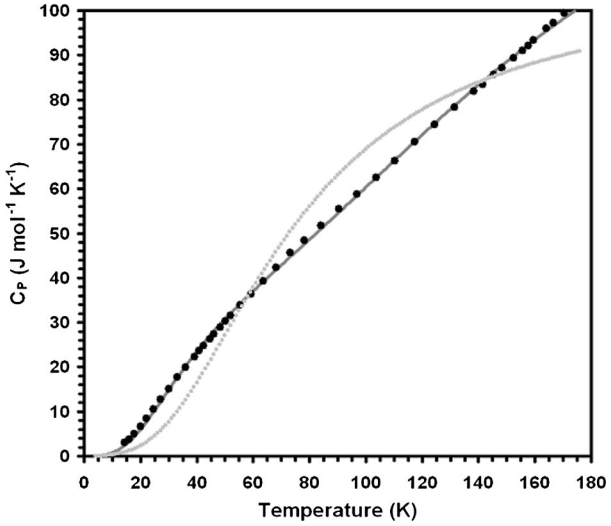

FIG. 5. Isobaric heat capacity, C_P, of ADH as a function of temperature. Filled circles are the measurements of Chan and Giauque (Ref. 3). The dashed line represents the best possible fit of a Debye model with a single Debye temperature. The solid line is the fit of a model with two characteristic Debye temperatures [Eq. (3)].

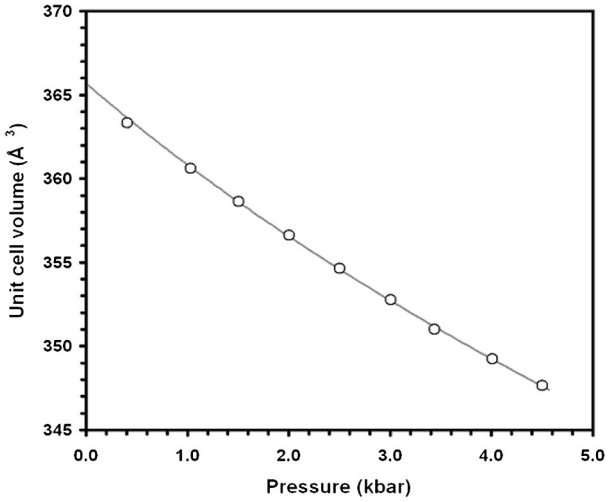

FIG. 6. Plot of refined unit cell volume against pressure at 174 K. The solid line is a third order Birch–Murnaghan equation of state.

to C_V values, which have not been measured. Furthermore, with respect to the analysis of our thermal expansion data, we are fitting to C_P data for *hydrogenous* ADH, rather than *deuterated* ADH, wherein the isotopic shift of vibrational frequencies will lead to different Debye temperatures. Nevertheless, this approximation is far superior to the single Debye model fit [Eq. (2)]. The parameters resulting from the fitting of Eq. (3) (yielding the solid line in Fig. 5) to C_P values are; $\theta_D^A = 165 \pm 3$ K, $\theta_D^B = 729 \pm 4$ K, $X = 0.181\,22 \pm 0.004\,18$, and $Y = 0.477\,46 \pm 0.010\,66$. This result is of interest because it shows that the heat capacity of ADH I does not approach the classical high temperature limit of Dulong and Petit ($3nk_B$), but instead trends towards $\sim 2nk_B$. The two Debye temperatures correspond to vibrational wave numbers of, respectively, 115 and 507 cm^{-1}; these probably represent translational and rotational excitations of the water molecules in ADH.[2]

Equation (1) is now refitted to the $V(T)$ data using the double-Debye model, with $E(T)$ fixed from fitting Eq. (3) rather than having θ_D as a free variable. The elastic parameters resulting from this fit are considerably more sensible: $V_{0,0} = 356.464 \pm 0.005$ Å^3, $(K_{0,0}/\gamma) = 7.163 \pm 0.024$ GPa, and $K'_{0,0} = 5.41 \pm 0.33$. It would be useful to extract independent values for $K_{0,0}$ and γ from this fit, and a model-dependent approach by which these may be determined is presented in Sec. III C.

Previous studies[5,10] have estimated the unit cell volume as a function of temperature using an equation of the form

$$\frac{1}{V(T)} = \frac{1}{V_0} \exp\left[-\left(\frac{A}{B+1} \right) T^{B+1} \right], \tag{4}$$

where V_0 is the unit cell volume at zero Kelvin and A and B are parameters. The volume coefficient of thermal expansion, α_V, is therefore given by Eq. (5).

$$\alpha_V = AT^B. \tag{5}$$

For comparison with earlier work, and to provide a very simple means of calculating the density of ADH I as a function of temperature, we have fitted Eq. (4) to our $V(T)$ data. The resulting fit yields $V_0 = 356.391 \pm 0.011$ Å^3, $A = 1.1825 \pm 0.0053 \times 10^{-6}$, and $B = 1.0662 \pm 0.0097$. The fit is excellent above ~ 50 K, but becomes increasingly poor below this temperature as the thermal expansivity changes from a roughly linear dependence on T to a T^3 dependence. Nevertheless, the maximum difference from our measured volumes does not exceed 0.3% at 4.2 K. Hence, Eq. (4) is more than adequate for determining densities in planetary interiors for example.

The final observation we make with regard to the thermal expansivity is in relation to other compounds in the ammonia–water system. The thermal expansivity of ADH I is $\sim 300 \times 10^{-6}$ K^{-1} at the melting point (176 K); this is approximately double the volume thermal expansivity of ice

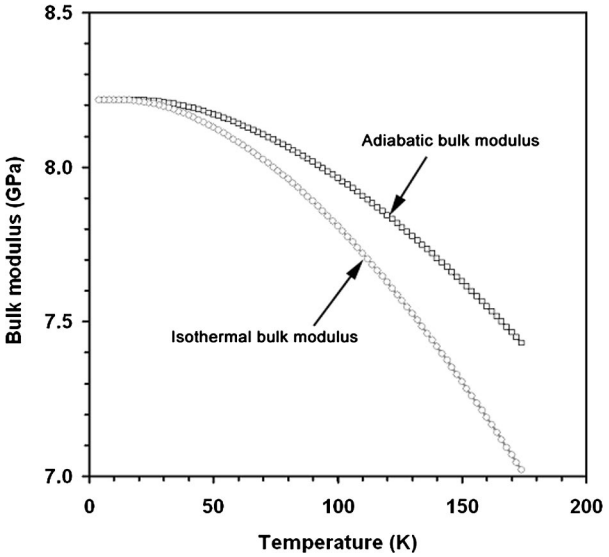

FIG. 7. The temperature dependencies of the adiabatic bulk modulus, K^S, and the isothermal bulk modulus, K^T, determined by assuming a temperature invariant Grüneisen ratio.

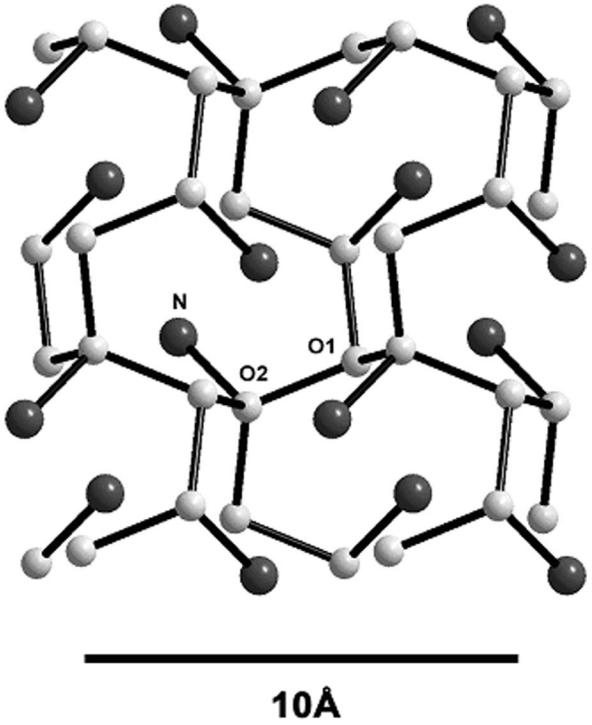

FIG. 8. The heavy atom framework in ADH I. Light gray spheres are oxygen atoms, dark gray spheres are nitrogen atoms.

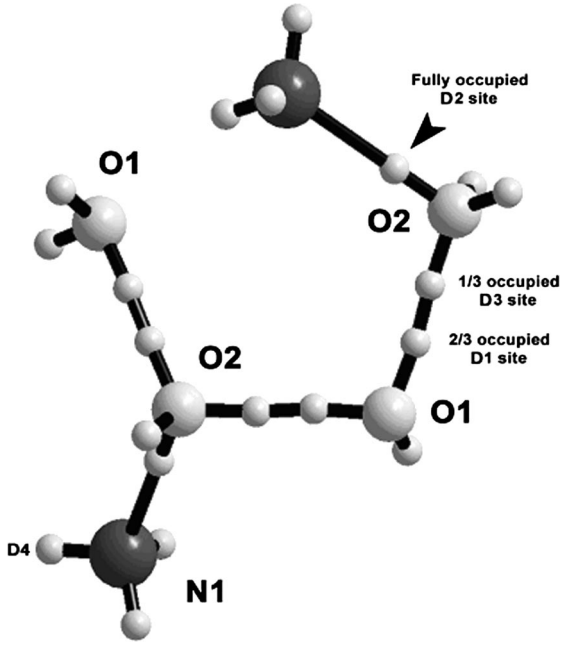

FIG. 9. The arrangement of partially occupied deuterium sites in ADH I. Atomic designations refer to those given in Table I.

Ih close to its melting point,[27] and roughly 60% of the thermal expansivity of solid ammonia near its melting point.[28] Since we were also able to extract cell parameters for the low-pressure phase of ammonia monohydrate (AMH I), which occurred as an accessory phase, we can confirm that its thermal expansivity is very similar to ADH I. To be more precise, the density of AMH I as a function of temperature is well fitted by Eq. (5) with the parameters A and B identical to those for ADH I; V_0 for deuterated AMH I takes the value 242.260 ± 0.020 Å^3.

The experimental low-temperature molar volumes of both ADH I and AMH I can be compared with our earlier computational results.[5,29] The calculated unit cell volumes of ADH I and AMH I in the athermal limit are 350.4 ± 0.7Å^3 and 242.0 ± 0.5 Å^3, respectively. Hence the calculated volume of ADH I is in error ($\Delta V/V$) by $-1.7 \pm 0.2\%$, and that of AMH I by $-0.1 \pm 0.3\%$; results which we consider to be excellent.

B. Incompressibility

Diffraction patterns for ADH I were collected at nine pressure points from 0.041 to 0.45 GPa along the 174 K isotherm and refined to yield the unit cell volume (Fig. 6). These data were fitted with a third-order Birch–Murnaghan equation of state (BMEOS) to yield the following parameters: Zero pressure unit cell volume, $V_{0,174} = 365.69 \pm 0.16$ Å^3, zero pressure isothermal bulk modulus, $K_{0,174} = 7.02 \pm 0.25$ GPa, and the first pressure derivative of the bulk modulus, $K'_{0,174} = 9.56 \pm 1.28$. Note that these parameters are referenced to a temperature of 174 K. The fitted EOS is shown by the solid line in Fig. 6.

The Bragg peaks due to ice Ih were also refined to yield unit cell parameters as a function of pressure and fitted with a third-order BMEOS having $V_{0,174} = 129.02 \pm 0.06$ Å^3, $K_{0,174} = 9.69 \pm 0.64$ GPa, and $K'_{0,174} = 6.71 \pm 3.96$. These parameters are in excellent agreement with literature values for D_2O ice Ih at this temperature: $V_{0,175} = 128.99 \pm 0.01$ Å^3 and $K_{0,175} = 9.45 \pm 0.52$ GPa.[27,30]

The incompressibility of ADH I will become larger at lower temperatures; using ice Ih as an analog,[31,32] one might expect K_0 to become stiffer by ~ 1.2 GPa from 174 K down to absolute zero: i.e., the estimated incompressibility of deuterated ADH at 0 K is ~ 8.2 GPa (see also Sec. III C). Our calculated bulk modulus for hydrogenous ADH I in the athermal limit is 10.7 ± 0.5 GPa.[5] After correcting for the 1.7% error in V_0 (see Sec. III A), our modified K_0 is ~ 9.7 GPa. Hence the estimated 0 K value for deuterated ADH I is 1.5 GPa (or $\sim 15\%$) smaller than the calculated value, a perfectly reasonable difference to attribute purely to the differing strengths of hydrogen versus deuteron bonds. In both glacial ammonia and water ice the bulk moduli of the deuterated solids are significantly smaller than those of the hydrogenous solids.[30,33] At 90 K, the isothermal bulk modulus of ND_3 is 15% smaller than for NH_3, and the difference increases with falling temperature.[33] Similarly, the isothermal bulk modulus of D_2O is 2.6% smaller than for H_2O at 145 K.[30] Again, the difference becomes larger at lower temperature, and may be as much as 10% at absolute zero. Based on these experimentally observed differences we conclude that our corrected first principles calculations[5] actually reproduce the incompressibility of hydrogenous ADH I very well indeed. Brillouin scattering studies of $NH_3 \cdot 2H_2O$ and $ND_3 \cdot 2D_2O$ crystals would resolve this question.

The first pressure derivative of the bulk modulus, $K'_{0,174}$, is quite large (9.56 ± 1.28), which is typical for a very soft material near to its melting point, and will become smaller as

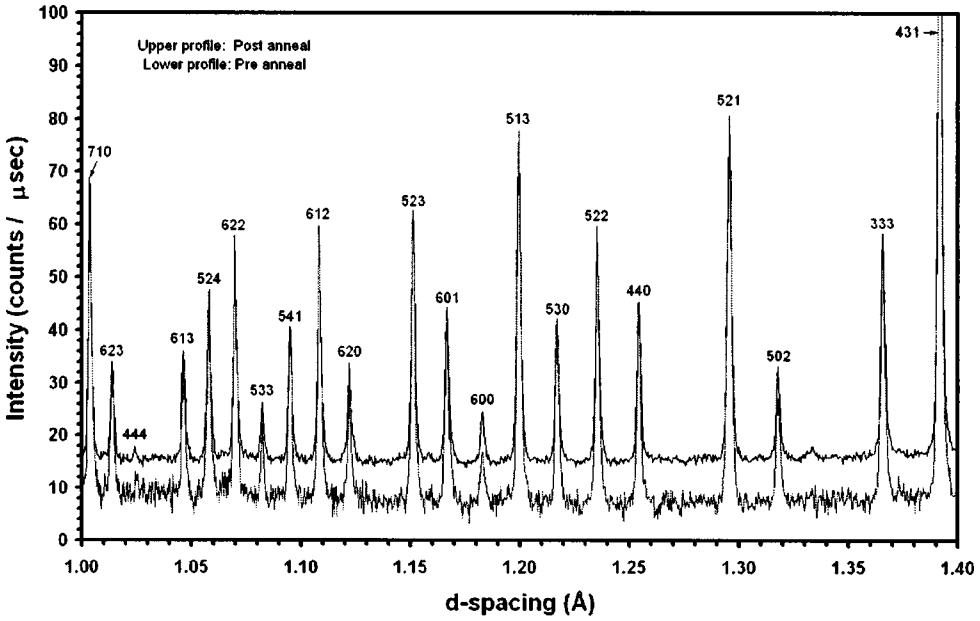

FIG. 10. Diffraction patterns acquired at 40 K from the pre-annealed ADH I sample, and from the sample annealed at 120 K for 36 hours. There is no discernible difference in the peak widths between the two patterns which would be indicative of strain broadening following a partial ordering transformation.

the crystal is cooled and it stiffens. Our calculated value of $K'_{0,0}=5.44\pm0.19$,[5] agrees very well with the value of $K'_{0,0}=5.41\pm0.33$ reported in Sec. III A derived from the fitting of Eq. (1) with two Debye temperatures.

C. The Grüneisen ratio and adiabatic bulk modulus

Thermodynamic quantities, such as C_V and C_P, are related to elastic properties, such as the isothermal bulk modulus, K^T, or the adiabatic bulk modulus, K^S, by the Grüneisen ratio, γ, according to Eqs. (6) and (7),

$$\gamma=\frac{\alpha_V K^T V_m}{C_V}=\frac{\alpha_V K^S V_m}{C_P}, \tag{6}$$

$$\frac{C_P}{C_V}=\frac{K^S}{K^T}=(1+\alpha_V\gamma T). \tag{7}$$

Our neutron diffraction measurements provide values for the molar volume, V_m, as well as α_V and K^T at 174 K. We can employ the previously measured values[3] of C_P to solve for the unknowns, C_V, K^S, and γ. The calculated values of these parameters at 174 K are thus $C_V=94.603\ \mathrm{J\,mol^{-1}\,K^{-1}}$, $K^S=7.415$ GPa, and $\gamma=1.148$. This value for the Grüneisen ratio is interesting because substituting it into the result for $(K_{0,0}/\gamma)=7.163$ GPa, as found in Sec. III A, yields $K_{0,0}=8.224$ GPa. This is very close to the incompressibility at zero Kelvin we estimated in Sec. III B by assuming that ADH stiffens at the same rate as ice Ih. Hence, it is reasonable to postulate a model in which γ is temperature invariant and thus estimate $K^T_{0,T}$ and $K^S_{0,T}$. Figure 7 shows the temperature dependencies of K^T and K^S found by assuming $\gamma=1.148$ from 0 to 176 K.

D. The crystal structure

The structure of ADH I (Fig. 8) consists of two crystallographically distinct water molecules hydrogen bonded into a three dimensional zeolite-like network. This network has large open channels within which ammonia molecules are sited. At high homologous temperatures, the water molecules are known to be orientationally disordered,[4] and this is described using partially occupied deuteron sites, as shown in Fig. 9. Hence ADH I is an isotropic glassy crystal.

We proposed that ADH I should undergo an ordering transition to an antiferroelectric structure at $\sim$140 K, resulting in a lowering of symmetry from $P2_13$ to $P2_12_12_1$.[5] This appeared to be supported by some experimental evidence as discussed in Ref. 5.

However, during the pre-annealing data collection, no evidence of such a transition was observed. At all temperatures from 174 K down to 4.2 K the observed diffraction pattern was well fitted by the disordered structure. The refined structure at 4.2 K is given in Table I. The sample was subsequently held at 120 K for 36 hours and examined further during warming from 40 to 160 K. Again, the observed structure was that of the cubic disordered phase at all temperatures. No sign of ordering below the predicted transition temperature was seen. Indeed, as Fig. 10 shows, there is no significant difference between the pre-annealing diffraction pattern and the post-annealing diffraction pattern at 40 K.

Clearly the transition to the ordered phase (which, thermodynamically, *must* be more stable than the disordered phase at zero pressure and temperature) is frustrated by kinetics. The transition apparently takes place at a temperature where the configurational freedom (the mobility of the deuterons) is negligible; i.e., much below 140 K, and probably below 100 K. This is the same phenomenon which frustrates the ordering transition in pure ice Ih.[34] The question remains, however, ''What is responsible for some of the experimentally observed changes near 140 K in, for example, the dielectric properties?'' We have observed no microscopic explanation for these changes.

A full set of isotropic structure refinements were carried

out on the post-annealing data set. These can be obtained from the Electronic Physics Auxiliary Publishing Service (EPAPS).[35]

IV. SUMMARY

We have completed the first detailed neutron powder diffraction study of deuterated ammonia dihydrate across the full range of pressure and temperature conditions under which the low-pressure phase is stable (0–176 K at ambient pressure, and 0–0.45 GPa at 174 K). This has allowed us to determine the full thermal equation of state of ADH I, providing values for the thermal expansivity, incompressibility, and the functional dependence of the internal energy on temperature. Our earlier first-principles calculations are found to be in agreement with these experimental results. These properties can be used to place constraints on evolutionary models of large icy moons in the outer Solar System.

The transition to an ordered crystal was kinetically hindered on the time scale of our experimental study, but might run to partial completion with further annealing (perhaps several hundred hours at $\sim$50 K) and perhaps with a suitable dopant. Certainly, on the surface of icy planets, one might expect timescales of order 10^9 years to be adequate for the formation of ordered ADH.

ACKNOWLEDGMENTS

The authors wish to thank the ISIS facility for beam time to conduct these experiments, and Support Staff for technical assistance during our time on HRPD. A.D.F. acknowledges a grant from the UCL Graduate School in support of this work. L.V. gratefully acknowledges receipt of a Royal Society University Research Fellowship.

[1] A.-P. Rollet and G. Vuillard, C. R. Acad. Sci. URSS **243**, 383 (1956).
[2] J. E. Bertie and M. R. Shehata, J. Chem. Phys. **81**, 27 (1984).
[3] J. P. Chan and W. F. Giauque, J. Phys. Chem. **68**, 3053 (1964).
[4] J. Loveday and R. J. Nelmes, in *Science and Technology of High Pressure: Proceedings of AIRAPT-17*, edited by M. H. Manghnani, W. J. Nellis, and M. T. Nicol (Universities Press, Hyderabad, India, 2000), pp. 133–136.
[5] A. D. Fortes, I. G. Wood, J. P. Brodholt, and L. Vočadlo, Icarus **162**, 59 (2003).
[6] J. S. Lewis, Icarus **16**, 241 (1972).
[7] M. L. Johnson and M. Nicol, J. Geophys. Res. **92**, 6339 (1987).
[8] J. S. Kargel, Icarus **100**, 556 (1992).
[9] G. J. Consalmagno, Icarus **64**, 401 (1985).
[10] S. K. Croft, J. I. Lunine, and J. S. Kargel, Icarus **73**, 279 (1988).
[11] R. M. Ibberson, W. I. F. David, and K. S. Knight, RAL-92-031, Rutherford Appleton Laboratory, Oxfordshire, U.K. (1992): http://www.isis.rl.ac.uk/crystallography/hrpd
[12] D. L. Hogenboom, J. S. Kargel, G. J. Consolmagno, T. C. Holden, L. Lee, and M. Buyyounouski, Icarus **128**, 171 (1997).
[13] J. Loveday, S. M. Guthrie, and R. J. Nelmes, ISIS Facility Experimental Report (POLARIS) RB 9859. Rutherford Appleton Laboratory, RAL-TR-1999-050 (1999).
[14] J. Yarger, J. I. Lunine, and M. Burke, J. Geophys. Res. **98**, 13109 (1993).
[15] O. Mishima, Nature (London) **384**, 546 (1996).
[16] E. L. Gromnitskaya, O. V. Stal'gorova, V. V. Brazhkin, and A. G. Lyapin, Phys. Rev. B **64**, 094205 (2001).
[17] J. D. Londono, J. L. Finney, and W. F. Kuhs, J. Chem. Phys. **97**, 547 (1992).
[18] G. S. Pawley, J. Appl. Crystallogr. **14**, 357 (1981).
[19] *Profile Analysis of Neutron Powder Diffraction Data*, RAL-92-032 Rutherford Appleton Laboratory, Oxfordshire, U.K. (1993).
[20] A. C. Larson and R. B. Von Dreele, LAUR 86-748, Los Alamos Laboratory (1994).
[21] S. W. Peterson and H. W. Levy, Acta Crystallogr. **10**, 70 (1957).
[22] J. D. Londono, W. F. Kuhs, and J. L. Finney, J. Chem. Phys. **98**, 4878 (1993).
[23] D. C. Wallace, *Thermodynamics of Crystals* (Dover, New York, 1998).
[24] N. W. Ashcroft and N. D. Mermin, *Solid State Physics* (Harcourt Brace College, Orlando, Florida, 1976).
[25] L. Vočadlo, K. S. Knight, G. D. Price, and I. G. Wood, Phys. Chem. Miner. **29**, 132 (2002).
[26] I. G. Wood, K. S. Knight, G. D. Price, and J. A. Stuart, J. Appl. Crystallogr. **35**, 291 (2002).
[27] K. Röttger, A. Endriss, J. Ihringer, S. Doyle, and W. F. Kuhs, Acta Crystallogr., Sect. B: Struct. Sci. **50**, 644 (1994).
[28] V. G. Manzhelii and A. M. Tolkachev, Fiz. Tverd. Tela (Leningrad) **8**, 1035 (1966).
[29] A. D. Fortes, J. P. Brodholt, I. G. Wood, L. Vočadlo, and H. D. B. Jenkins, J. Chem. Phys. **115**, 7006 (2001).
[30] U. Mitzdorf and D. Helmreich, J. Acoust. Soc. Am. **49**, 723 (1971).
[31] G. Dantl, J. Phys.: Condens. Matter **7**, 390 (1968).
[32] T. M. Proctor, J. Acoust. Soc. Am. **39**, 972 (1966).
[33] E. I. Voitovich, A. M. Tolkachev, and V. G. Manzhelii, J. Low Temp. Phys. **5**, 435 (1971).
[34] H. Suga, Thermochim. Acta **300**, 117 (1997).
[35] See EPAPS Document No. E-JCPSA6-119-501344 for isotropic refinements of the crystal structure of ADH I from the post-annealing data set. A direct link to this document may be found in the online article's HTML reference section. The document may also be reached via the EPAPS homepage (http://www.aip.org/pubservs/epaps.html) or from ftp.aip.org in the directory /epaps/. See the EPAPS homepage for more information.